Stanisław STRZELECKI[*], Krzysztof KUMYCZ[**]

THE EFFECT OF OIL GROOVES ON THE STATIC CHARACTERISTICS OF CYLINDRICAL 3-LOBE JOURNAL BEARINGS

WPŁYW ROWKÓW SMAROWYCH NA CHARAKTERYSTYKI STATYCZNE CYLINDRYCZNEGO ŁOŻYSKA 3-POWIERZCHNIOWEGO

Key words:

theory of hydrodynamic lubrication, multilobe journal bearings, oil grooves

Słowa kluczowe:

teoria smarowania hydrodynamicznego, łożyska ślizgowe, rowki smarowe

Summary

Multilobe journal bearings with three operating lobes with cylindrical profiles and separated by oil grooves are applied in different types of rotating machinery. The design of 3-lobe journal bearings in relation to the number of lobes and oil grooves affects bearing static characteristics.

[*] SIMLOGIC. Automation Solution Center, Lodz, Poland, e-mail: stanislaw.strzelecki@p.lodz.pl.
[**] Research Development Centre of Textile Machinery POLMATEX-CENARO, Lodz, Poland, e-mail: serwis@cenaro.com.pl.

This paper describes the results of the calculations of static characteristics of 3-lobe cylindrical journal bearings in relation to the different angular widths of oil grooves. The bases for the static characteristics are the oil film pressure, temperature, and viscosity distributions. The iterative solution of oil film geometry, Reynolds, energy, and viscosity equations are used to determine the required distributions and the load capacity of bearings. Laminar, adiabatic oil film, and the static equilibrium position of journal were assumed.

INTRODUCTION

The systems of the journal bearings of modern rotating machinery are characterised by the application of multilobe bearings **[L. 1–8]**. These types of bearings can be manufactured with the bore of different profiles, e.g., cylindrical or pericycloid. Exemplary applications of such bearings are turbines, turbo-generators **[L. 1–5]**, or grinding machines **[L. 9, 10]**. The design of bearings and particularly the number of lobes and oil grooves affects the bearing operation and its static and dynamic characteristics. Static characteristics of journal bearings are determined by oil film pressure, temperature, viscosity distributions, the minimum oil film thickness its maximum pressure and temperature, oil flow, and friction loss **[L. 3–6]**. In the case of multilobe journal bearings, higher friction losses and lower load capacity with the increase in the lobe number can be expected **[L. 1–3]**.

The 3-lobe bearing can be characterised by the symmetrical or asymmetrical arrangement of lobes, which are separated by the oil grooves. In each case, the oil grooves' length and extent (i.e. angular width) play very significant roles in the cooling of the oil film and varying the bearing characteristics. The 3-lobe classic bearing is designed as three parts with cylindrical non-continuous profiles **[L. 3, 6]**. Individual lobes of this bearing are designed as the arc of the circle with the centre points placed on the symmetry line of the single lobe. In the symmetric multilobe bearing, the circle inscribed in the bearing profile is tangent to the lobe exactly at the middle point of each lobe.

In case of 3-lobe cylindrical journal bearing, the radius of each lobe is equal to the radius of a circle inscribed in the bearing profile. A very important feature of cylindrical 3-lobe bearings **(Fig. 1**) is simple manufacturing, which decreases the total costs of the bearing system. However, to obtain the most efficient design, the effect of oil grooves on the performances of 3-lobe cylindrical bearing needs more investigation.

Reliable and durable operation of rotating machinery depends on the sophisticated and adequate process of the computation of the bearing and bearing system **[L. 1–6].** The code of computation allows one to determine the bearing characteristics and the effect of oil grooves on performance **[L. 1, 5]**.

This paper presents a theoretical investigation into the effect of the angular width of oil grooves on the static characteristics of 3-lobe cylindrical journal bearings. The Reynolds, energy, and viscosity equations were solved numerically based on the assumption of incompressible lubricant, and the laminar and adiabatic flow of oil in the lubricating gap of finite length bearing. The static equilibrium position of the journal was assumed in the calculations. Finite difference method was applied for the solution of all hydrodynamic equations.

GEOMETRY OF OIL FILM

The geometry of the oil film gap of multilobe journal bearings **(Fig. 1)** is described by Equation (1).

$$\overline{H}(\varphi) = \overline{H}_{Li}(\varphi) - \varepsilon \cdot \cos(\varphi - \alpha), \tag{1}$$

Where: $\overline{H}(\varphi)$ – dimensionless oil film thickness ($\overline{H} = h / \Delta R$),
h – oil film thickness (m),
ΔR – radial clearance,
$\Delta R = R_b - r$, (m), R_b – bearing bore diameter (m),
r – journal radius (m),
α – attitude angle, (^{0}),
ε – relative eccentricity $\varepsilon = e/\Delta R$,
e – journal eccentricity (m),
φ – peripheral co-ordinate, (^{0}).

The first member of the right side of Equation (1), i.e. $\overline{H}_{Li}(\varphi)$, that determines the gap geometry of multilobe journal bearings (3LM), at the concentric position of journal and bearing axis, has the following form **[L. 1–3]**:

$$\overline{H}_{Li}(\varphi) = \psi_{si} + (\psi_{si} - 1) \cdot \cos(\varphi - \gamma_i) \tag{2}$$

Where: R – bearing lobe radius, (m),
ψ_s – lobe relative clearance,
$\psi_s = (R - r)/\Delta R$ γ_i – angle of lobe centre point, (^{0}).

In case of multilobe, cylindrical (3LC) journal bearings, the lobe relative clearance is assumed as $\psi_{si} = 1$. Lobe angle γ_i (i =1, 2, 3) is placed opposite to the respective lobe, e.g. $\gamma_2 = 90^0$ for the lobe No. 2 **(Fig. 1a).**

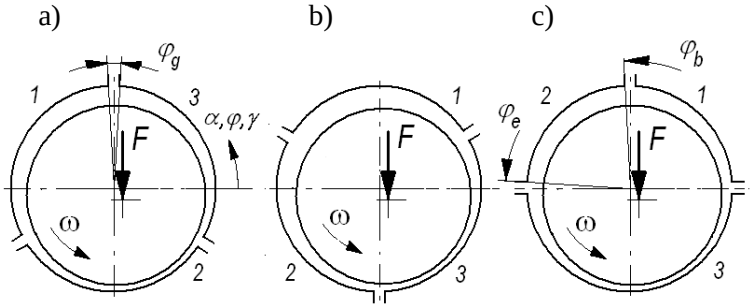

Fig. 1. Cylindrical 3-lobe journal bearings; a – symmetrical 3LOL, b – symmetrical 3LBL, c – asymmetrical 3LOL; LOL – load *F* on the lobe, LBL – load *F* between lobes, φ_g – angular width of oil groove, φ_b, φ_e – angle of the begin and end of lobe

Rys. 1. Łożyska ślizgowe cylindryczne 3-powierzchniowe; a – symetryczne 3LOL, b – symetryczne 3LBL, c – asymetryczne 3LOL; LOL – obciążenie *F* na segment, LBL – obciążenie *F* między segmentami, φ_g – szerokość kątowa rowka smarowego, φ_b, φ_e – kąt początkowy i końcowy segmentu

STATIC CHARACTERISTICS OF BEARING

The oil film pressure distribution, which is one of the static characteristics, was calculated from the following general dimensionless Reynolds equation **[L. 1–5]:**

$$\frac{\partial}{\partial\varphi}\left(\frac{\overline{H}^3}{\overline{\eta}}\frac{\partial\overline{p}}{\partial\varphi}\right)+\left(\frac{D}{L}\right)^2\frac{\partial}{\partial\overline{z}}\left(\frac{\overline{H}^3}{\overline{\eta}}\frac{\partial\overline{p}}{\partial\overline{z}}\right)=6\frac{\partial\overline{H}}{\partial\varphi}+12\frac{\partial\overline{H}}{\partial\phi}, \tag{3}$$

Where: D, L – bearing diameter and length (m), e – journal eccentricity (m), p – oil film pressure, (MPa), $\overline{p}$ – dimensionless oil film pressure, $\overline{p}=p\cdot\psi^2/\eta\cdot\omega$, $\overline{z}$ – dimensionless axial coordinate, ψ – bearing relative clearance, ψ = ΔR/r, η – dynamic viscosity of oil, (Ns/m^2), ω – angular velocity (1/s), $\overline{\eta}$ – dimensionless viscosity of oil, $\overline{\eta}=\eta/\eta_o$, η_o – dynamic viscosity at ambient temperature (Ns/m^2), ϕ – dimensionless time, $\phi=\omega\cdot t$, t – time (sec).

Oil film pressure, temperature and viscosity fields were obtained by solving Equation (3) together with energy and viscosity equations **[L. 1–5]**. The pressure boundary condition assumes positive values of oil film pressure only and ambient pressure on the sides of bearings. The oil film temperature $\overline{T}(\varphi,\overline{z})$ on the bearing edges ($\overline{z}$ = ±1) was computed by means of parabolic approximation **[L. 5].** The integrated oil forces on the shaft and bearing act

through their respective centres, which are, in the direction of the load, a distance apart, and there will be a couple sets of magnitudes, which correspond to a frictional forces at the surface of the shaft. For the calculation of the friction loss and oil flow in the bearing gap **[L. 3, 6]**, it is necessary to consider the peripheral υ_φ and longitudinal υ_z velocity distributions that are given by Equations (4) and (5):

$$\upsilon_\varphi = \frac{1}{2\eta r}\frac{\partial p}{\partial \varphi}\left[(y')^2 - y'\cdot h\right] + \frac{\omega \cdot r}{h}y' \,, \tag{4}$$

$$\upsilon_z = \frac{1}{2\eta}\frac{\partial p}{\partial z}\left[(y')^2 - y'\cdot h\right], \tag{5}$$

with y' varying in the range <0,h> and η – dynamic viscosity of oil, (Ns/m^2).

The distribution of the tangential stress τ in the lubricant is governed by

$$\tau = \eta \frac{\partial \upsilon_\varphi}{\partial y'} \tag{6}$$

The resistance to flow was calculated on the assumption that the lubricating gap is completely filled with an oil of similar properties in the state of laminar flow **[L. 1–3]**; therefore, Equation (6) can be assumed to hold everywhere in the bearing gap. Substitution of Equation (4) into Equation (6) and integrating the tangential forces acting on the journal surface (y'= 0) gives the dimensionless friction loss $\overline{F_r}$ expressed by Equation (7):

$$\overline{F_r} = -\frac{1}{4}\int_{-1}^{+1}\int_{0}^{2\pi}\left(\frac{\overline{H}}{2}\frac{\partial \overline{p}}{\partial \varphi} + \frac{\overline{\eta}}{\overline{H}}\right)d\varphi d\overline{z} \,. \tag{7}$$

The oil volume flowing through the bearing is determined by

$$q_{fl} = 2\int_{0}^{2\pi}\int_{0}^{h}(\upsilon_z)_{z=\pm\frac{L}{2}}\, y'\cdot dh \cdot d\varphi \,. \tag{8}$$

Introducing Equation (5) into Equation (8) gives the oil flow in non-dimensional terms

$$\overline{q}_{fl} = \frac{1}{192}\int_{\varphi_b}^{\varphi_e}\frac{1}{\overline{\eta}}\left[\overline{H}^3\frac{d\overline{p}}{dz}(2+\psi\cdot\overline{H})\right]_{\overline{z}=\pm 1} d\varphi . \tag{9}$$

Equation (7) and Equation (9) were applied in the developed code of numerical calculations of friction losses and the oil flow of the considered bearings.

RESULTS OF CALCULATIONS

The calculations included the non-dimensional load capacity *So* (*So* – Sommerfeld number, $So = F\cdot\psi^2/(L\cdot D\cdot\eta\cdot\omega)$ where: F – resultant force of oil film (N)), journal displacement ε, static equilibrium position angles α_{eq}, oil flow $\overline{q}_{fl}$, friction losses $\overline{F}_r$, maximum oil film temperature T_{max}. The 3-lobe cylindrical journal bearings under consideration have the length to diameter ratio L/D = 0.8 and L/D = 1.0. The rotational speed of journal was n = 3000 rpm. The feeding oil temperature was 40^0C and the corresponding thermal coefficients K_T **[L. 1, 5]** were 0.045 and 0.014 at the bearing relative clearances ψ = 1.5‰ ψ = 2.7‰, respectively. Exemplary results of the calculations of oil film pressure and temperature distributions at different angular widths of oil grooves φ_g are showed in **Fig. 2** and **Fig. 3**. Journal displacement ε, static equilibrium position angles α_{eq}, maximum oil film temperature T_{max}, oil flow $\overline{q}_{fl}$ and friction losses $\overline{F}_r$ versus Sommerfeld number S_0 are presented in **Fig. 4** through **Fig. 10. Fig. 11** shows the measured temperatures in the 3-lobe pericycloid journal bearings of a grinder spindle **[L. 9, 10**].

Oil film pressure and temperature distributions show a decrease with the increase in the oil groove angular width φ_g (**Fig. 2** and **Fig. 3**) on all lobes of the bearing, indicating a point supply hole of an infinitely small radius.

The journal displacements ε and static equilibrium position angles α_{eq} of different multilobe bearings can be observed in **Fig. 4** and **Fig. 5**. In the case of bearings with the lobe relative clearance ψ_s = 1, the displacements are larger with a larger Sommerfeld number as compared to the bearing with the lobe relative clearance ψ_s = 1.5 or ψ_s = 3.0 **(Fig. 4)**. An increase in the lobe relative clearance at assumed journal eccentricity ε causes the decrease in the Sommerfeld number **(Fig. 4).** The static equilibrium position angles α_{eq} for all types of operating surfaces (i.e. at ψ_s = 1.0 and ψ_s = 1.5 and ψ_s = 3.0) are presented in **Fig. 5**.

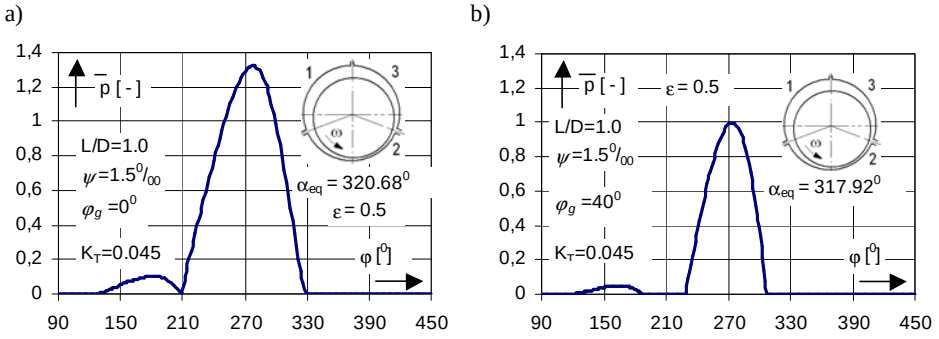

Fig. 2. Oil film pressure distribution in cylindrical 3-lobe journal bearing; a) - point supply, $\varphi_g = 0^0$ and b) -angular width of oil grooves $\varphi_g = 40^0$

Rys. 2. Rozkłady ciśnienia w cylindrycznym łożysku 3-powierzchniowym; a) z punktowym zasilaniem, $\varphi_g = 0^0$ oraz b) z rowkiem smarowym o rozwartości $\varphi_g = 40^0$

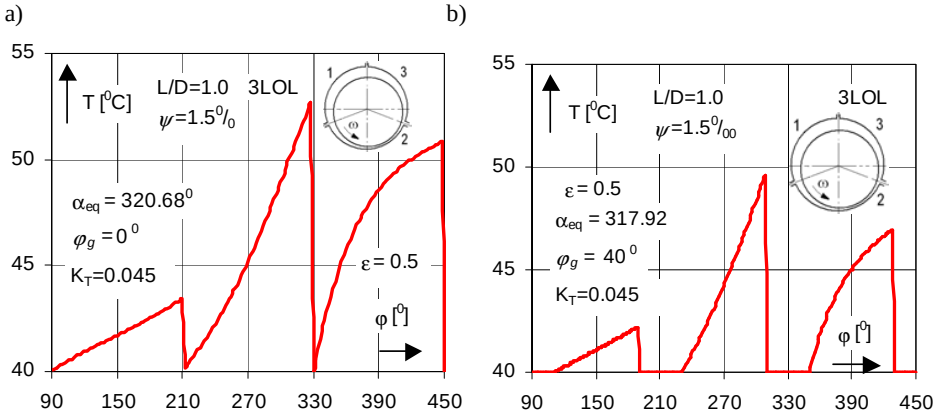

Fig. 3. Oil film temperature distribution in cylindrical 3-lobe journal bearings; a) point supply, $\varphi_g = 0^0$, and b) oil groove angular width $\varphi_g = 40^0$

Rys. 3. Rozkłady temperatury w cylindrycznym łożysku 3-powierzchniowym; a) zasilanie punktowe $\varphi_g = 0^0$ oraz b) rowek smarowy o rozwartości $\varphi_g = 40^0$

The journal displacements ε and static equilibrium position angles α_{eq} for different angular widths φ_g of oil grooves are presented in **Fig. 6** and **Fig. 7**. At an assumed value of relative eccentricity ε or static equilibrium position angle α_{eq}, there is a decrease in Sommerfeld number S_0 with the increase in the angular width of oil groove (e.g. **Fig. 6a** or **Fig. 7a**, respectively).

The effect of groove angular width φ_g on the maximum oil film temperature T_{max} is presented in **Fig. 8**. At bearing relative clearance $\psi = 1.5‰$ and for Sommerfeld numbers larger that 0.7, an increase in the groove angular width φ_g causes the increase in maximum temperature; however, at S_0 smaller

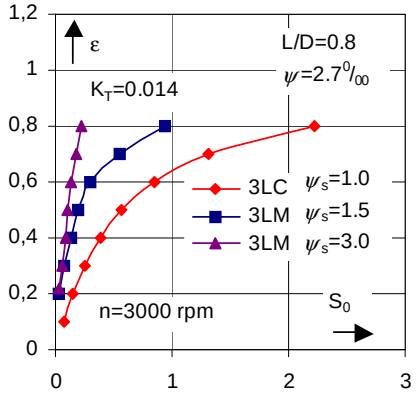

Fig. 4. Load capacity versus Sommerfeld
Rys. 4. Nośność w funkcji liczby Sommerfelda

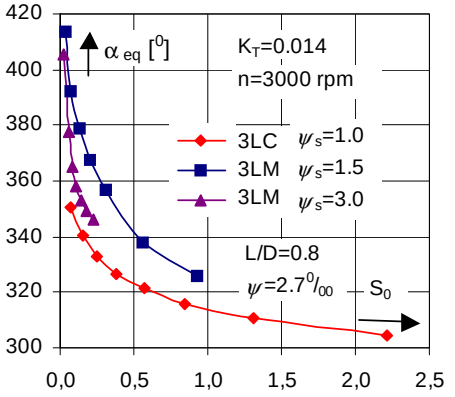

Fig. 5. Static equilibrium position angles number versus Sommerfeld number
Rys. 5. Kąty statycznego położenia równowagi w funkcji liczby Sommerfelda

a) b)

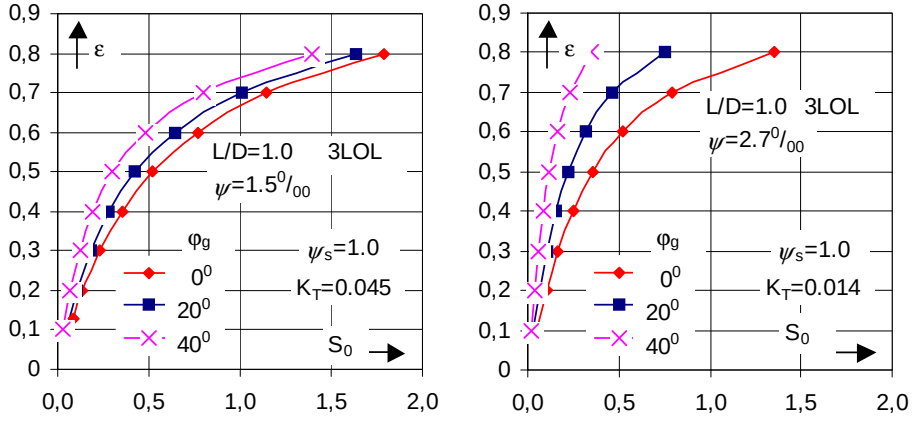

Fig. 6. Journal displacements in relation to different values of relative clearance: a) 1.5‰, b) 2.7‰
Rys. 6. Przemieszczenie czopa dla różnych wartości luzu względnego: a) 1,5‰, b) 2,7‰

than 0.7, there is a decrease in the T_{max} at the increase in oil groove extent **(Fig. 8a)**. However, at larger relative clearance, i.e. ψ = 2.7‰, maximum oil film temperature T_{max} increases with the angular width of groove from Sommerfeld number S_0 at about 0.1 **(Fig. 8b)**.

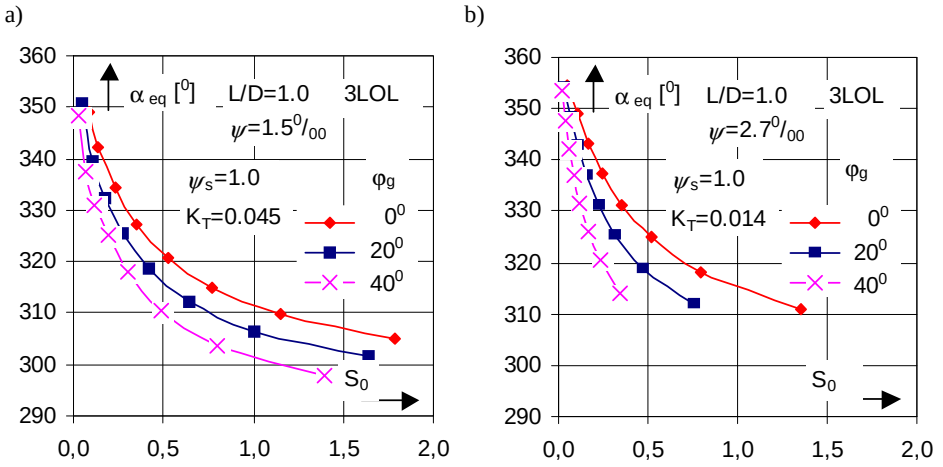

Fig. 7. Static equilibrium position angles in relation to different values of relative clearance a) 1.5‰, b) 2.7‰

Rys. 7. Statyczne kąty położenia czopa 3 dla różnych wartosci luzu względnego: a) 1,5‰, b) 2,7‰

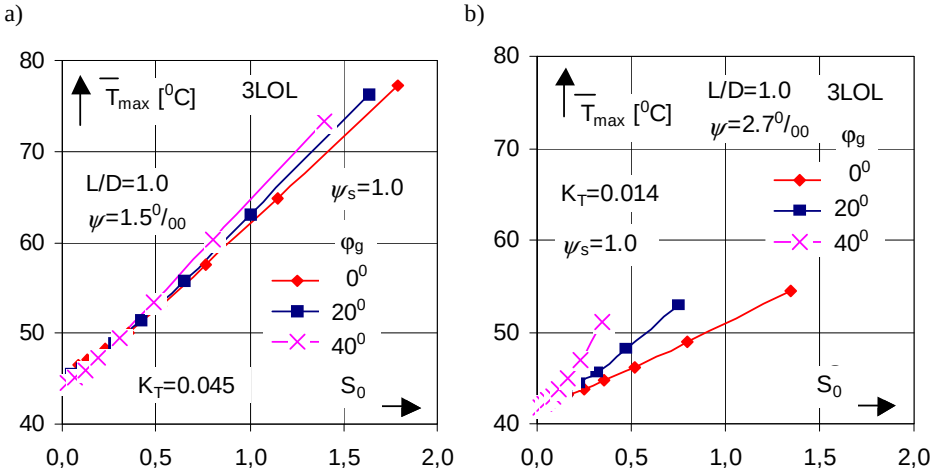

Fig. 8. Maximum oil film temperature in relation to the relative clearance: a) 1.5‰, b) 2.7‰

Rys. 8. Maksymalna temperatura filmu smarowego dla luzu względnego: a) 1,5‰, b) 2,7‰

Oil flow $\overline{q}_{fl}$ decreases with the increase in groove width **(Fig. 9a** and **9b)**, and a larger decrease in oil flow exists with larger values of Sommerfeld numbers S_0 (e.g., **Fig. 9a** and S_0 larger than 0.1).

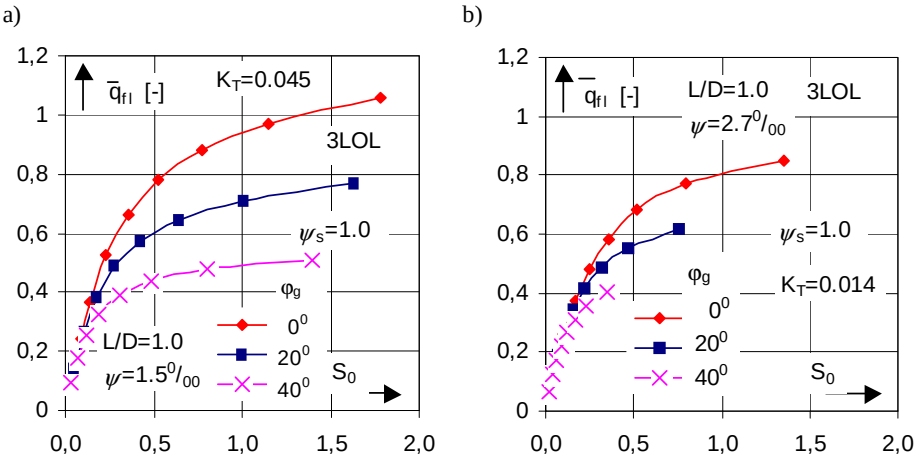

Fig. 9. Oil flow versus So in relation to different values of relative clearance: a) 1.5‰, b) 2.7‰

Rys. 9. Przepływ oleju w funkcji liczby Sommerfelda dla różnych wartości luzu względnego: a) 1,5‰, b) 2,7‰

Friction losses $\overline{F_r}$ show a decrease with the increase in the oil groove extent φ_g at assumed value of Sommerfeld number S_0 for both considered values of bearing relative clearances **(Fig. 10a** and **10b).**

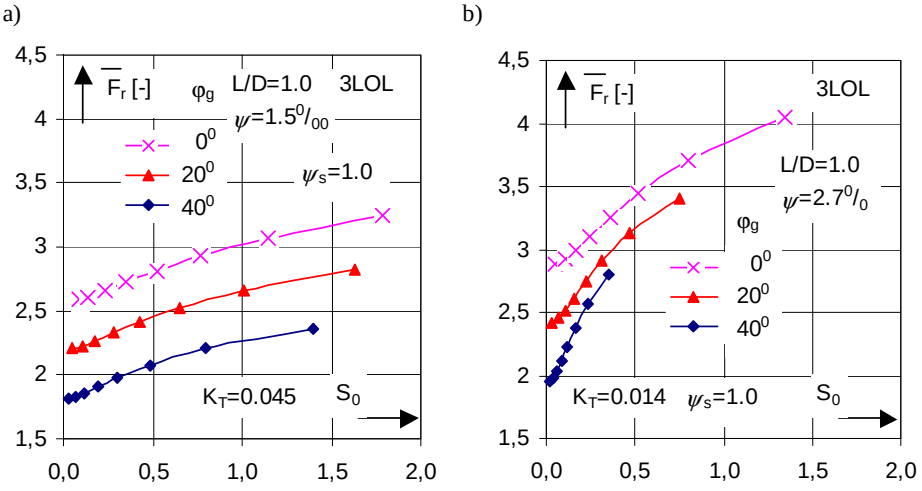

Fig. 10. Friction losses in relation to different values of relative clearance: a) 1.5‰, b) 2.7‰

Rys. 10. Straty tarcia dla różnych wartości luzu względnego: a) 1,5‰, b) 2,7‰

Fig. 11 presents the results of temperature measurements on the operating surfaces of 3-lobe pericycloid journal bearings applied in the bearing system of a grinder spindle **[L. 9, 10]**. After about 3 hours, there is very small increase in the measured temperatures (**Fig. 11,** thermocouples Numbers 4, 5, 6), and these values were compared to the computed ones **(Table 1) [L. 9, 10].** The differences in temperature values certify the correctness of the model that was assumed and the results of the calculations.

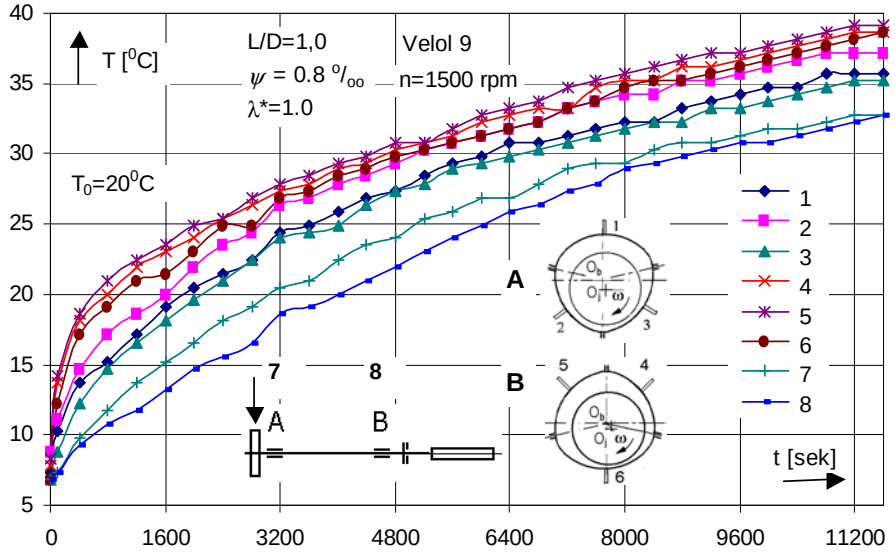

Fig. 11. Ranges of temperatures measured on the operating surfaces of 3-lobe pericycloid journal bearings of the grinder spindle – 1 through 8 thermocouples, 7 and 8 thermocouples of sleeve casings [L. 9, 10]

Rys. 11. Przebiegi temperatur mierzonych na powierzchniach roboczych łożyska 3-powierzchniowego z zarysem perycykloidalnym wrzeciennika szlifierki; 1 do 8 czujniki temperatury, 7 i 8 czujniki temperatury obudowy łożysk **[L. 9, 10]**

Table 1. Calculated and measured maximum temperatures
Tabela 1. Wyniki obliczeń i pomiarów maksymalnych temperatur

No of thermocouple	T_{max} [^{0}C]		
	Calculation	Experiment	Difference
4	34	38	4
5	48	39	9
6	42	38.5	3.5

CONCLUSIONS

Investigations into the effect of oil grooves' angular width on the static characteristics of 3-lobe cylindrical journal bearings lead to the conclusions given below.

1. Oil film pressure and temperature distributions show the decrease in relation to the increase in the oil groove angular width on all lobes of the bearing.
2. At assumed value of relative eccentricity ε or static equilibrium position angle α_{eq}, there is a decrease in Sommerfeld number S_0 in relation to the increase in the angular width of oil grooves.
3. Oil flow decreases in relation to the increasing angular width of oil grooves, and it is more evident in relation to larger values of Sommerfeld numbers.
4. Friction losses show a decrease in relation to the increase in the angular width of grooves in relation to the assumed value of the Sommerfeld number for the considered bearing relative clearances.
5. Temperatures measured in 3-lobe pericycloid journal bearings of a grinder spindle are close to the temperatures computed for cylindrical 3-lobe journal bearings.

REFERENCES

1. Han D.C.: Statische und dynamische Eigenschaften von Gleitlagern bei hohen Umfangsgeschwindigkeiten und bei Verkanntung Diss. TU Karlsruhe. Karlsruhe 1979.
2. Dimofte F.: Wave Journal Bearing with Compressible Lubricant- Part I: The Wave Bearing Concept and a Comparison to the Plain Circular Bearing. Tribology Transaction, Vol. 38, 1995, 153–160.
3. Pinkus O.: Thermal Aspects of Fluid Film Tribology. ASME PRESS. New York 1990.
4. Boncompain R., Fillon M., Frene J.: Analysis of Thermal Effects in Hydrodynamic Bearings. Journal of Tribology, Vol. 108, 1986, 219–224.
5. Ghoneam S.M., Strzelecki S.: Thermal Problems of Multilobe Journal Bearings. Meccanica. DO1 10.1007/s11012-006-9004-z. 41, Springer 2006, 571–579.
6. Strzelecki S.: Design of the tribosystem of 3-lobe journal bearing. Tribologia R. 28 nr 4, 1997, 323–332.
7. Gethin D.T., Medwell J.O.: An experimental investigation into the thermohydrodynamic behaviour of a high speed cylindrical bore journal bearing. ASME Transactions. Journal of Tribology, Vol. 107, 1985, 538–543.
8. Strzelecki S., Spalek J.: Thermal Effects in Cylindrical Journal Bearings of High Speed Gearbox. Lubrication Science, Vol. 15, No. 1, 2002, 17–33.
9. Strzelecki S., Socha Z.: Effect of Load Direction on the Oil Film Temperature Distribution of 3-Lobe Pericycloid Journal Bearing. Technical University Ostrava. PIME2009. Trans. of Tech. Univ. Ostrava. Metallurg. Ser. 2009, R. 52, No. 3, 2009, 211–216.

10. Strzelecki S., Socha Z.: Effect of feeding oil pressure on the oil film temperature of 3-lobe pericycloid bearing. INTERTRIBO 2009, October 21-23.2009. Slovak Republik, Proceedings of the Conference, 2009, 33–36.

Streszczenie

Układy łożyskowe maszyn wirnikowych charakteryzują się stosowaniem łożysk wielopowierzchniowych [L. 1–8]. Konstrukcja łożyska, w tym liczba powierzchni roboczych, rowków smarowych i ich szerokość kątowa wpływają na jego charakterystyki statyczne i dynamiczne. Charakterystyki statyczne obejmują rozkłady ciśnienia, temperatury, lepkości filmu smarowego, minimalną grubość, maksymalną temperaturę i ciśnienie w filmie smarowym, przepływ środka smarowego oraz straty tarcia.

Program obliczeniowy charakterystyk łożyska umożliwia wyznaczenie charakterystyk statycznych łożyska, m.in. wpływ wielkości rowków smarowych na charakterystyki łożyska.

Przedstawiono wyniki badań teoretycznych wpływu kątowej szerokości rowka smarowego na charakterystyki statyczne 3-powierzchniowego, cylindrycznego łożyska ślizgowego. Równania Reynoldsa, energii i lepkości rozwiązano metodą różnic skończonych, zakładając laminarny, adiabatyczny przepływ środka smarowego w łożysku o skończonej długości oraz statyczne położenie równowagi czopa